

SLIDING FRICTION BETWEEN AMORPHOUS COTTON FIBER AND CHROMIUM SURFACES: A MOLECULAR DYNAMICS STUDY

ZHE YAN,* KAIXIANG JIANG,* PENGWEI FAN,* WENJUAN FANG,* CUNZHOU ZHU,*
PENG PAN,* HUI CAO** and YOUQIANG ZHANG*

*School of Mechanical and Electrical Engineering, Key Laboratory of Modern Agricultural Engineering, Tarim University, Alar 843300, China

**State Key Laboratory of Tribology, Tsinghua University, Beijing 100084, China

✉ Corresponding author: Y. Q. Zhang, zhangyqlzjd@126.com

Received November 29, 2021

It is challenging to experimentally determine the micro-friction mechanism of cotton fiber and metal in the sliding process. The influence of load and temperature on the interface behavior during dry friction between amorphous cotton fiber and chromium, the contact interface evolution and friction coefficient are studied using reactive molecular dynamics. The simulation results show that chromium–oxygen bonds are formed on the contact interface of the friction system during the sliding process. Furthermore, the relationship between friction coefficient, temperature, and load varies with the mechanical state of cotton cellulose. The relationship is positive when the cotton cellulose is in the glassy state. However, when cotton cellulose is in a highly elastic state, its friction coefficient is negatively related to the load. This study systematically evaluated the effects of temperature and load on the slip process from the atomic scale, provided a reason for the wear of the hard materials of the friction pair, and provided theoretical support for the study of this type of friction mechanism.

Keywords: cotton cellulose, chromium, molecular dynamics, dry friction, mechanochemical reactions

INTRODUCTION

Cotton fiber has good ecological benefits as a natural material, and its products are widely used in all aspects of life.¹⁻² However, during the entire processing of cotton fibers, different machine parts pull, drag, wind, and rub the cotton fibers on their surface until they are arranged in the desired shape or form. This friction behavior controls the quality of textile products, the efficiency of yarn processing, twisting, and winding,³ causing continuous friction between the cotton fiber and the surface of the processing equipment components, resulting in the breakage, entanglement of the cotton fiber bundle, and the wear and deformation of the metal surface component. As chromium metal has excellent properties, such as hardness, brittleness and corrosion resistance,⁴ it is widely used as the outer layer and functional coating of protective and decorative coating systems. It has always occupied an important position in the electro-

plating industry. Therefore, most of the friction between cotton fiber and metal is between cotton fiber and chromium. This typical “the hard worn by the soft” friction behavior leads to the wear failure of hard materials, which inevitably affects the stability, long life, and reliability of metal parts and increases economic costs.

The friction process of cotton fiber has been extensively studied by experiments. For instance, A. Hussain *et al.*⁵ evaluated the surface roughness, coefficient of friction, and tensile properties of cotton fabrics. The results demonstrate that the coefficient of friction can vary with the fabric pattern and that an increase in surface roughness increases the fiber’s friction, while reducing its tensile properties. K. Eshkobilov *et al.*⁶ proposed a molecular-mechanical-electrical theory of interaction in contact state in the process of studying the interaction between polymer materials and raw cotton, combining with modern wear theory. Hosseinali *et al.*⁷ used a slip friction

tester to study the friction properties of fiber components from different cotton varieties. The results show that the friction characteristics of cotton fibers vary from species to species. Zhang *et al.*⁸ studied the mechanical self-locking of cotton fibers on metal surfaces with different textures through traditional processing methods. Although the successful application of microelectromechanical systems (MEMS) and nanoelectromechanical systems (NEMS) devices have made significant progress in the study of cotton fiber tribology, the influence on the evolution of interfacial particles and friction behavior under the coupling of load and temperature is still unclear. The unique physical and chemical structure of cotton fiber determines the particularity and arduousness of studying its tribological behavior. The phenomenological theory of friction interface and the subsurface area is still lacking, and there are still ambiguities in fiber friction experiment technology and interpretation of fiber friction results. At the same time, in cotton fiber friction research, most experiments are focused on the friction between fiber groups rather than on the friction between individual fibers. It is a challenge to study this kind of friction mechanism fundamentally.

Load and temperature are the two most critical mechanical parameters that affect friction.⁹ The friction between cotton fiber and metal is dynamic, and its atomic details cannot be observed in experiments. Because of the lack of atomic details, the nano-scale friction mechanism between cotton fiber and metal under the coupling of load and temperature has not been well understood. However, with the continuous development of science and technology, computational simulation is more and more capable of accurately predicting physical phenomena, and numerical simulation methods have become commonly used in nano research. Among others approaches, molecular dynamics (MD) simulations have become one of the most important methods for studying friction and wear, and it has also made the research of nano-scale polymer friction a trend nowadays. At the micro-level, MD simulations have provided information that is not easy to obtain from experimental analysis and have helped to understand better atomic-scale details of the materials structure and properties.^{10,11} For instance, Muthoka *et al.*¹² established an all-atom model and used GROMACS software combined with OPLS-AA force fields to simulate the molecular dynamics of cellulose I nanofibers under

equilibrium conditions to study the properties and structural stability of cellulose I nanofibers. J. A. Sánchez-Badillo *et al.*¹³ used a kinetic approach to study the solvent behavior of cellulose I β crystallites through atomic interactions and degrees of deviation. The results show that the deviation change is related to the pH parameter of the solution. Huang *et al.*¹⁴ studied the properties of cellulose I β at different temperatures by molecular dynamics method, and the results showed that the pyrolysis was divided into three steps.

On the other hand, first-principles simulations¹⁵ can accurately describe the interface structure of friction systems at the electronic scale. Unfortunately, due to computational cost issues, only a small number of atoms or molecules can be simulated on the picosecond time scale, which is challenging to achieve the whole evolution of sliding friction system simulation. Nonetheless, for the classical MD simulation method, the number of atoms that can be simulated can reach tens of thousands, but usually requires predefined connections between atoms not to involve the simulation of chemical reactions. The reactive force fields (ReaxFF)¹⁶ were developed to circumvent the shortcomings between first principles and classical MD. ReaxFF enables molecular simulation to record the mechanical response during the simulation process and captures the formation and dissociation of chemical bonds at a relatively low computational cost. This method has been widely used to simulate materials' chemical and mechanical properties and the interaction of molecules between interfaces.¹⁷⁻¹⁸

In this article, using MD simulations, the continuous dry friction behavior of the interface between cotton cellulose and metal chromium is analyzed to shed light on the effect of cotton cellulose on the dry friction process with chromium. In addition, exploring the degradation mechanism and properties of metal friction pairs provides a specific basis for predicting the life and damage protection of metal parts.

MODELLING AND SIMULATION APPROACH

All atoms model and ReaxFF force field

The Prandl-Tomlinson and the united atom models have been widely used to simplify the smallest-scale friction problem and learn about the friction mechanisms.¹⁹⁻²⁰ However, they have low accuracy and some structural details cannot be

obtained, and there are many restrictions on the study of tribological mechanisms. Therefore, in this article, we use all-atom models in molecular modeling. The reactive force field²¹ (ReaxFF) used was developed by Duin *et al.* It is based on *ab initio* calculations and a semi-empirical potential obtained by combining Pauling's bond length and bond energy relationship. The parameters required for the systems studied here were taken from somewhere else.²²⁻²⁴ The reactive force field is composed of two parts: intraatomic interaction and interatomic interaction, *i.e.*, the potential energy of the force field includes bonding and non-bonding interactions. Among them, van der Waals interaction and electrostatic interaction energies belong to the non-bonding interaction potential energy. This treatment of non-bonded interactions allows ReaxFF to describe covalent, ionic, and intermediate materials, thereby significantly improving its transferability. The total energy of ReaxFF can be expressed as:

$$E_{system} = E_{bond} + E_{under} + E_{over} + E_{val} + E_{pen} + E_{tors} + E_{conj} + E_{vdWaals} + E_{Coulomb} \quad (1)$$

where E_{bond} is the covalent interaction energy, E_{under} and E_{over} are atom under/overcoordination, E_{val} is the bond angle interaction energy, E_{pen} is the compensation energy, E_{tors} is the dihedral torsion energy, E_{conj} is the bond binding energy, and $E_{vdWaals}$ is the van der Waals action energy, $E_{Coulomb}$ is electrostatic action energy.

In ReaxFF, the connection is determined by the bond sequence calculated from the distance between the atoms; in each iteration, the bond sequence is calculated based on the distance between two atoms and their local environment. The ReaxFF force field uses the bond order (BO)

to calculate the bond energy, bond angle energy, and dihedral angle energy. The relative strength of the bond. The bond level is shown in Equation (2), and the bond parameters needed for the equations are presented in Table 1.

$$BO_{ij} = \exp \left[P_{bo,1} \cdot \left(\frac{r_{ij}}{r_o} \right)^{P_{bo,2}} \right] + \exp \left[P_{bo,3} \cdot \left(\frac{r_{ij}^\pi}{r_o} \right)^{P_{bo,4}} \right] + \exp \left[P_{bo,5} \cdot \left(\frac{r_{ij}^{\pi\pi}}{r_o} \right)^{P_{bo,6}} \right] \quad (2)$$

MD simulation setups

Cellulose nanofibers are the most basic structure of all cellulose and are the basis for the composition of long cellulose chains. The monomer structure of cellulose molecules has been theoretically obtained, and a large number of cellulose monomers have been polymerized to form long-chain fibers. In the conformational analysis of polymers, Flory²⁵ mentioned that when the amorphous model is established, the geometry of the final equilibrium system is close to the original model. Only in the process of balancing the system can small and subtle changes be observed. Therefore, establishing an initial model for amorphous cellulose is very important.

β -D-glucosyl is composed of two identical conformations twisted by 180°. Because cellobiose is a saturated six-membered ring compound with "chair-like" coordination, the carbon atoms in the six-membered ring are not on the same plane. Instead, the glucosyl groups are connected through ordinary oxygen atoms (ester bonds) to form a long cellulose chain. As shown in Figure 1, it is a single long chain of amorphous cellulose.

Table 1
Bond parameters in the revised equations

Bond	D_E^σ	D_E^π	$D_E^{\pi\pi}$	P_{be1}	P_{be2}
C-C	156.5963	100.0397	80	-0.8157	-0.1
C-H	170.2316	0	0	-0.5931	1
H-H	156.0973	0	0	-0.1377	1
C-O	160.4802	105.1693	23.3059	-0.3873	-0.3174
O-O	60.1463	176.6202	51.143	-0.2802	-0.1239
H-O	180.4373	0	0	-0.8074	1

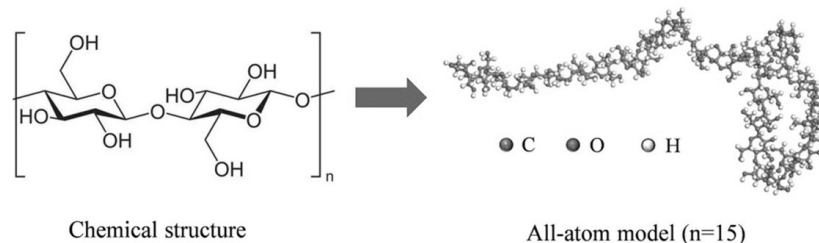


Figure 1: All-atom model of cellulose monomolecular chain

Table 2
Cotton cellulose model parameters in MD simulation

Chain length (DP)	30
Number of chains	3
Atomic number of the system	1260
Number of atoms in a supercell system	3780
Supercell structure size	30 Å × 30 Å × 34.079 Å

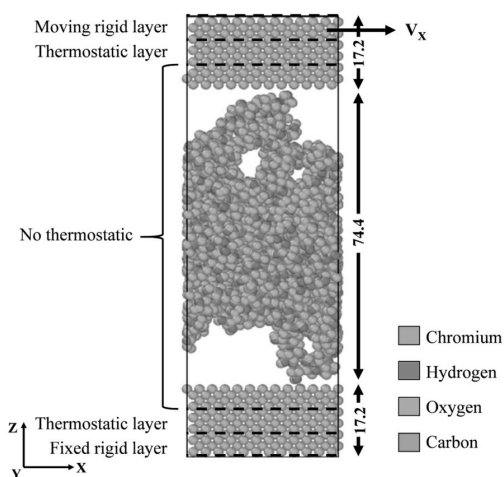


Figure 2: Molecular dynamics model of friction between amorphous cotton fiber and chromium metal surface

The study found that the physical and chemical properties obtained in the simulation process for different degrees of polymerization (DP) models are not significantly different.²⁶ Some scholars use cellulose chains with a DP of 20 to construct amorphous regions to study their mechanical properties. The results show that the simulation and experimental values are roughly the same.²⁷ When modeling the structure of amorphous cotton fibers, a random unit cell with a cellulose molecular chain arrangement density of 1.5 g/cm³ was chosen.²⁴ As a result, the cotton fiber model defines the cellulose molecular chains with chain length and chain number, as shown in Table 2.

The chromium unit cell structure is directly obtained from the Materials Studio software crystal material library.²⁸ First, the Cr(0 0 1)

surface was created, adding a vacuum space in the z-direction of the supercell. Next, the Cr(0 0 1) surface is exposed to cellulose because it is one of the most stable surfaces. To intuitively study the sliding friction process between cotton fiber and chromium, the chromium layer will maintain a smooth and flat surface, without special surface texture treatment.

The three-dimensional MD model of slip friction consists of a chromium layer of 3456 chromium atoms and an amorphous cellulose molecular chain. In friction and wear experiments, the size of the metal layer in the XY plane is usually larger than that of the cotton fiber part to make the constructed model closer to the actual slip friction experiment. In the model constructed in this paper, the size of the chromium layer in the XY plane (35 Å × 35 Å) is larger than that of

the middle layer cellulose molecular chain ($30 \text{ \AA} \times 30 \text{ \AA}$), and the initial size of the entire friction system is $35 \text{ \AA} \times 35 \text{ \AA} \times 110 \text{ \AA}$. To solve the problem of multiple slippages of cotton fiber on chromium metal by the boundary effect, the x and y directions of the model are set as periodic boundary conditions (PBC), and the z-direction is a non-periodic boundary. Figure 2 is a schematic diagram of the model system used in the study, composed of amorphous cotton cellulose and the Cr(0 0 1) surface. The multilayer structure is built up to the top of the simulation box in order. The quenched layer is kept at a constant temperature to dissipate the heat generated during the sliding process. Due to the force generated by the potential between the atoms, the atoms in the free layer can move freely.

In the friction simulation process, an external speed is applied to the slider, while pressure is applied to the rigid layer. The simulation consists of three steps: balance phase, pressure control phase, and friction phase, where external pressure and speed are applied. The top rigid layer compresses the central amorphous cotton fiber under constant pressure. Using the method described by Miller,²⁹ the atoms in the rigid layer are regarded as rigid bodies, and the normal loading pressure p (0.3 and 50.6 MPa) is applied to each chromium atom in the rigid body.³⁰ By the Langevin algorithm,³¹ the two thermally quenched layers are thermally scaled to the required temperature. Then, the free layer is set to micro-regular (NVE) integration and the speed and force of the fixed layer of the model are set to zero to fix the bottom of the model. To achieve a good structure for lateral friction simulation, it

takes a certain period loading simulation. Inheriting the optimized structure after loading balance, the slider moves linearly parallel to the y-direction. During the one-way sliding process, the speed v is set to 10.55 m/s along the one-way (1 0 0).³² All simulations use large-scale atomic/molecular parallel simulation (LAMMPS) software,³³ and post-processing of results uses OVITO software.³⁴

RESULTS AND DISCUSSION

Evolution of interface structure during the sliding process

When the metal slides on the cotton cellulose, it has a pronounced influence on the interface, but the evolution mechanism of the interface structure on the micro-nano scale is not clear yet. The interface structure evolution during the slip process at a speed of 10.55 m/s at 0.3 GPa and 50.6 GPa is shown in Figures 3 and 4, respectively (the values in Figures 3 and 4 are the total simulation time).

As shown in the atomic snapshot, the chromium metal layer is structurally complete in the initial slippage stage, as expected. However, as the slippage time increases, the long-chain atoms of cotton fibers embedded in the structure of the chromium matrix gradually increase, and the chromium matrix appears to suffer subsurface damage. Additionally, it was found that, under higher load and temperature, the wear and subsurface damage of the chromium matrix appear earlier, which can be confirmed by the evolution of the system's potential energy during the slip process, as shown in Figure 5.

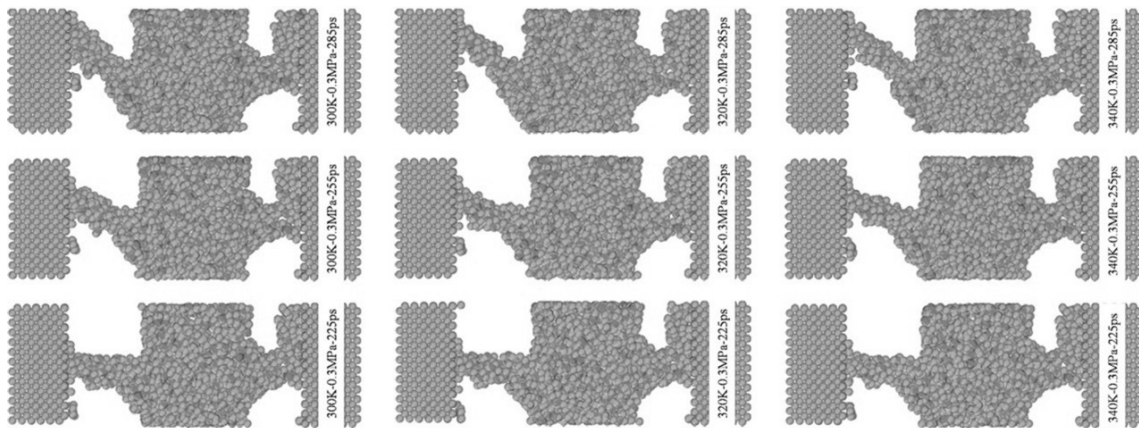


Figure 3: Evolution of interface structure during the sliding process at the initial temperature of 300 K, 320 K, and 340 K under 0.3 MPa

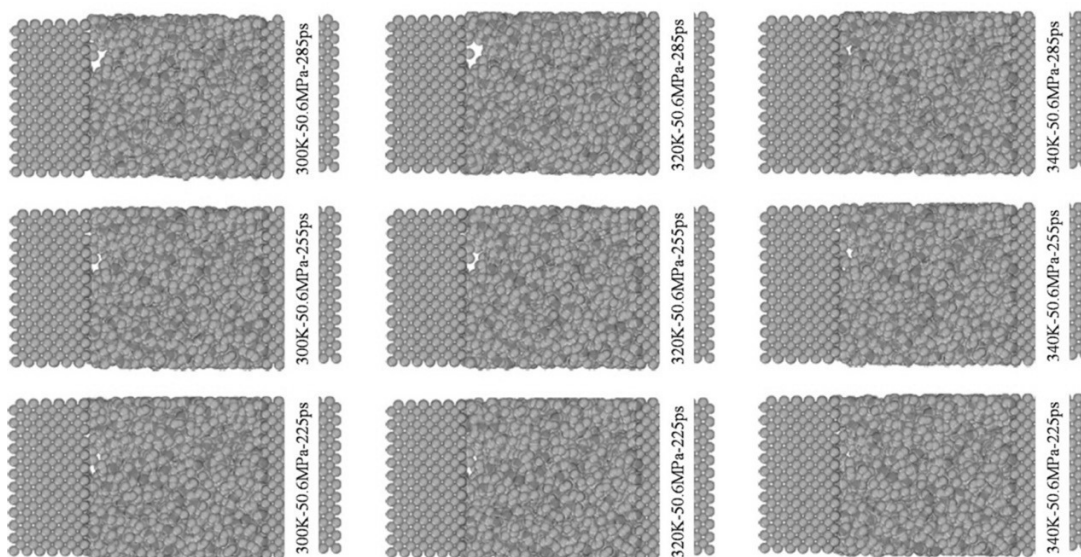


Figure 4: Evolution of interface structure during the sliding process at the initial temperature of 300 K, 320 K, and 340 K under 50.6 MPa

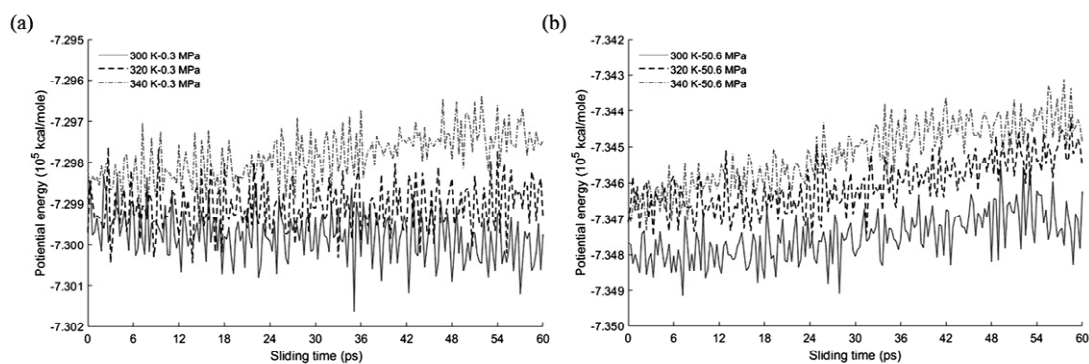


Figure 5: Evolution of potential energy in the process of friction sliding under different loads and temperatures

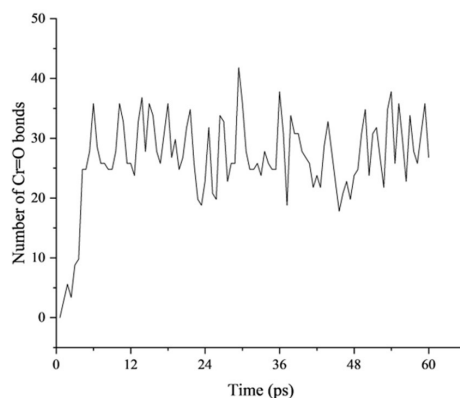


Figure 6: Number of Cr=O bonds during the friction simulation process

Furthermore, our data suggest that the selected temperature range has no significant effect on the chromium surface in the contact interface under different load conditions. However, under the

same load conditions, a higher temperature is more likely to cause more contact interface wear. To further explore the mechanism of chromium matrix surface damage during the sliding process,

the evolution of the number of atomic bonds in the model was analyzed. The Cr=O bond number of the sliding time interface under the conditions of 0.3 MPa and 300 K was calculated, as shown in Figure 6.

The simulation results show that during the sliding friction process, O atoms in the cotton cellulose structure combine with Cr to form double bonds. At the same time, to verify the formation of the Cr=O bond, the friction system under the conditions of 0.3 MPa and 300 K was taken as the object, and the chromium-oxygen atom bond was marked in the simulation snapshot, as shown in Figure 7.

To confirm this result, the slip process of the system is introduced in detail from the atoms' radial distribution function (RDF). The distribution of O atoms surrounding Cr atoms before and after the sliding friction simulation is shown in Figure 8. In the RDF figure, when the contact distance in the z-direction exceeds 1.7 Å, the $g(r)$ value between the rubbed Cr and O atoms

suddenly increases. It shows that under the sliding friction of external load, oxygen atoms near the Cr metal layer increase during the friction process. Figure 8b shows a comparison of the radial distribution of the last frame of the friction system under the same load under different temperature conditions. Additionally, when the contact distance in the z-direction exceeds 1.7 Å, the $g(r)$ value between Cr and O atoms begins to increase, and there is a certain fluctuation. It shows that in the sliding friction process more Cr atoms react with O atoms, due to the combined action of van der Waals and other forces.

In Figure 9, under different loads and temperatures, the highest peaks in the radial distribution of Cr and O in the last frame of the slip process both appear at 1.96 Å, indicating the existence of chromium-oxygen bonds (the sharp peaks at 1.96 Å correspond to the Cr=O length). The comparison found that the highest peak values under the two different loads are in the order of 300 K, 340 K, and 320 K.

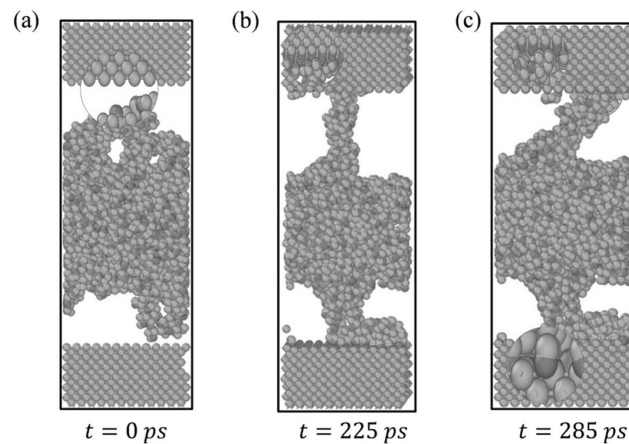


Figure 7: Atomistic simulation of amorphous cotton cellulose on the Cr(0 0 1) surface (a-c) (atomic snapshot of friction simulation at 0.3 MPa and 300 K)

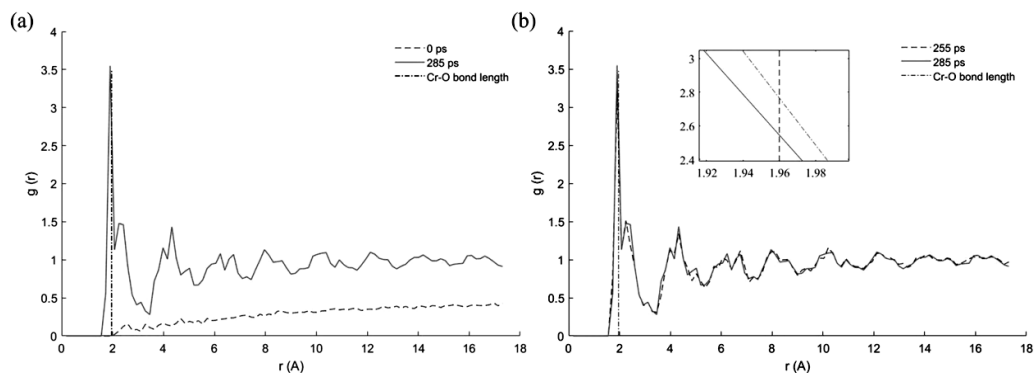


Figure 8: Radial distribution of Cr-O in a friction system at 300 K and 0.3 MPa at different time values

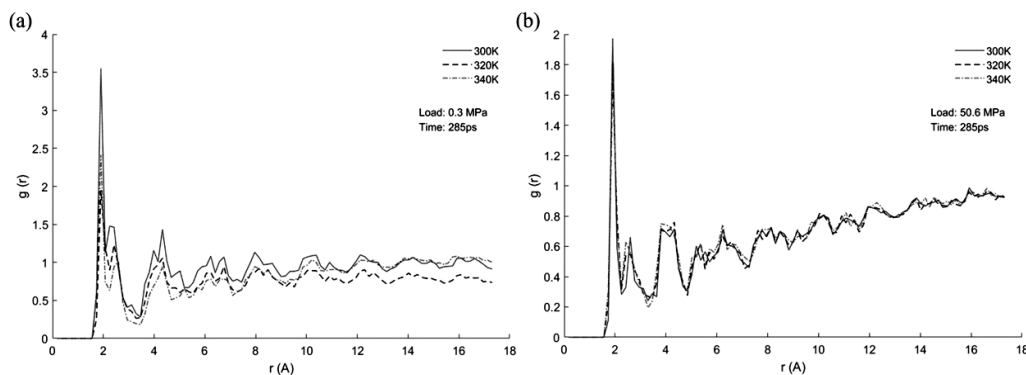


Figure 9: Radial distribution of the last frame of friction system slippage under different conditions

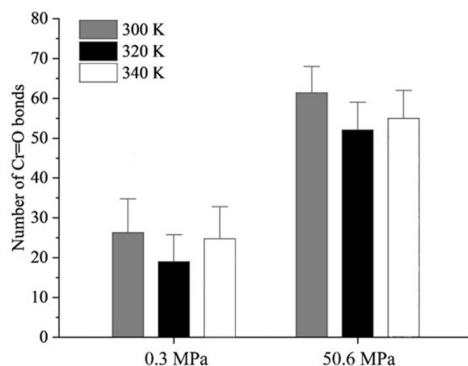


Figure 10: Number of Cr=O bonds in the chromium matrix during sliding under different loads and temperatures

It is worth noting that the peak range value of the low load is greater than that of the high load. This indicates that the radial distribution of chromium and oxygen in the friction system is sensitive to temperature and pressure under low load conditions. The histogram with the number of Cr=O bonds at 300 K, 320 K, and 340 K under two different loads during the sliding process is shown in Figure 10. Meanwhile, it can be seen clearly that the friction system under high load generates more chromium-oxygen bonds than the one under low load, and they all show a u-shaped distribution with the increase of temperature.

Effects of temperature on friction coefficient of sliding contact interface

The friction interface in the initial state of the friction system is not unevenly treated. Therefore, the magnitude of the friction coefficient indirectly determines the wear degree of the contact interface, and also indicates the degree of damage to the chromium layer. Because the friction coefficient is an instantaneous value, the average value of the friction coefficient within a certain range is taken as the corresponding time friction coefficient in the simulation process. Figure 11

shows the evolution of friction coefficient with sliding simulation time at different temperatures (the outermost rigid movable chrome layer of the friction system can apply different loads as required). The amorphous cotton fiber will show two different mechanical states: the glassy state and the high elastic state, as a function of temperature, in the temperature range of 300 K-340 K. Therefore, we will discuss the evolution of the friction coefficient in the same mechanical state (the T_g temperature of amorphous cellulose is 336 K).

As shown in Figure 11, under the same load conditions, when the amorphous cotton fiber is in the mechanical glassy state, the friction coefficient after stabilizing is positively correlated with temperature. However, with the increase of slip time, the friction system in the state of high elastic mechanics firstly decreases, then increases slightly, and finally becomes stable.

Effects of load on friction coefficient of sliding contact interface

Under different load conditions, the wear of the friction system is also different. Figure 12 shows the evolution of friction coefficient with

sliding simulation time under different loads.

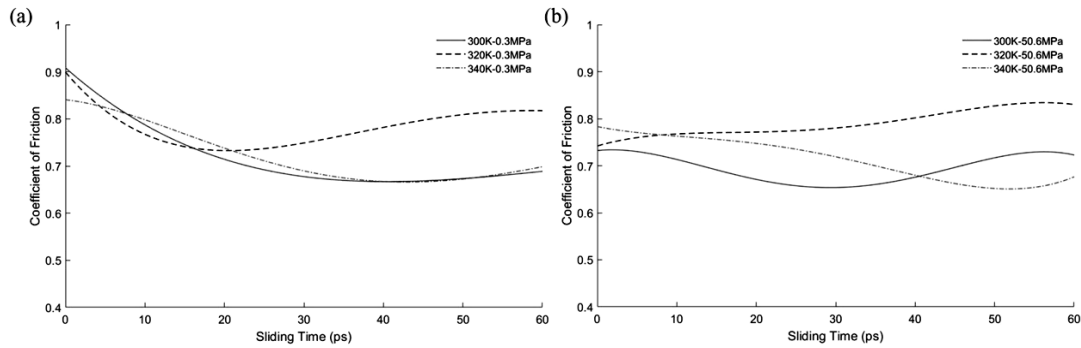


Figure 11: Variation of friction coefficient with sliding time under different temperatures (the curve in the figure is a higher-order fitting curve (the principle of least squares curve fitting) obtained by MATLAB solution, de-extreme value, and average value of 50 adjacent data)

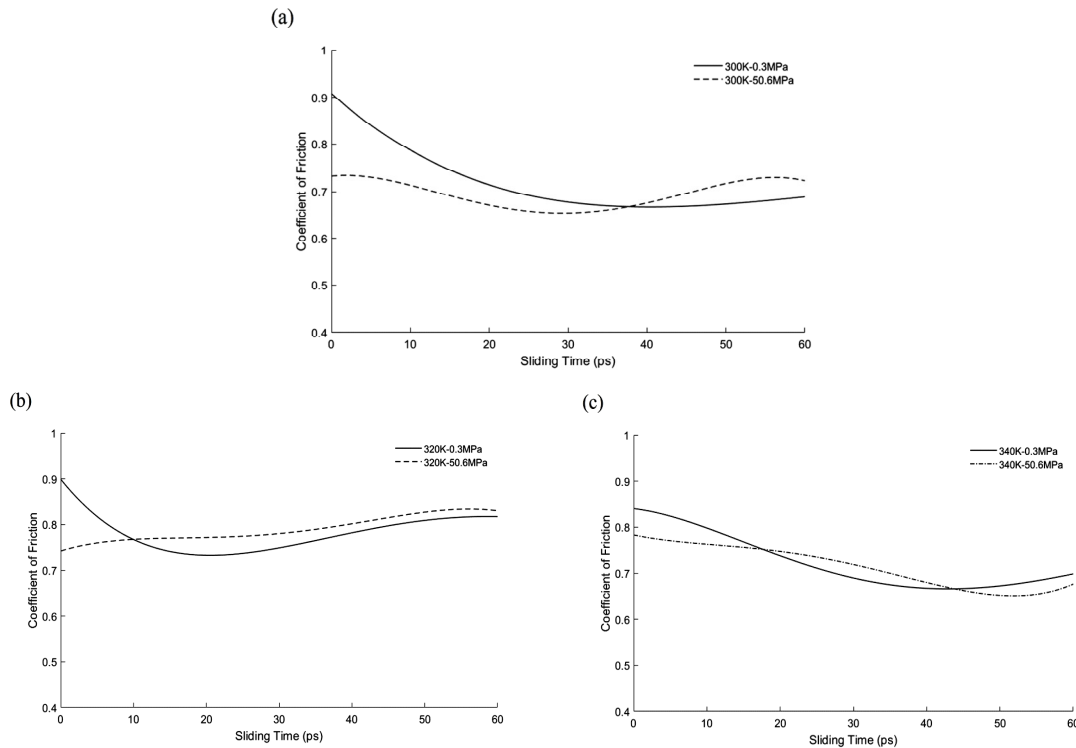


Figure 12: Variation of friction coefficient with sliding time under different loads

The results show that at the initial stage of the friction system slip, the decrease rate of the friction coefficient between the contact interface is larger under the condition of low load, which is caused by the decrease of the attraction between the molecules at the contact interface during the initial sliding process. As the slip continues, the interaction force between the molecules at the contact interface fluctuates dynamically and tends

to balance, and the corresponding friction coefficient also tends to be stable. In the stable state, the friction coefficient of the contact interface under high load is slightly higher than that under low load. On the other hand, the situation is opposite under the condition of a high elastic state. However, no matter what the mechanical state is, the difference in friction coefficient after stabilization is not large for

different loads, indicating that the influence of load on its friction coefficient is weakly correlated.

CONCLUSION

In this paper, the molecular dynamics method is used to study the effects of load and temperature on the dry friction slip between amorphous cotton cellulose and Cr(0 0 1) surface. Based on the visualization of the simulation process and comparative analysis of the number of Cr-O bonds and RDF curves before and after sliding, it is found that intermediate substances such as Cr-O bonds are generated during the sliding process of the friction system, which provides a further understanding of the friction and wear mechanism of “the hard worn by the soft”.

At the same time, the friction coefficient of amorphous cotton fiber and chromium metal sliding process under different temperatures and loads was also studied. The results show that the friction coefficients of amorphous cotton fibers are different when they are in different mechanical states. When cotton cellulose is in glassy state, the friction coefficient is positively related to temperature, and it is weakly related to load. When the load factor is involved, temperature plays a dominant role in the sliding process of the friction system. This study provides a theoretical basis for the different damage conditions of the contact interface between amorphous cotton cellulose and chromium metal, and provides a reference for the regulation of the tribological behavior of the interface between cotton cellulose and metal.

ACKNOWLEDGMENTS: This study was supported by the Xinjiang Production and Construction Corps Research Program (No. 2018AB007; No. 2021CB036). The authors are grateful to anonymous reviewers for their comments.

REFERENCES

- ¹ M. Zhang, Y. Tan and S. Liu, *J. Textile Sci. Eng.*, **38**, 68 (2021), <https://doi.org/10.3969/j.issn.2096-5184.2021.03.013>
- ² Y. Su and M. Ge, *J. Clothing Res.*, **3**, 9 (2018), <https://doi.org/10.3969/j.issn.1671-7147.2018.01.002>
- ³ W. Yu, “Textile Materials”, Beijing, China, Textile and Apparel Press, 2006

- ⁴ E. S. Ankuda, V. V. Kalmykov, M. V. Musokhranov and I. D. Sokolova, in *AIP Conference Proceedings*, AIP Publishing LLC, October 2021, vol. 2410, No. 1, p. 020005, <https://doi.org/10.1063/5.0068745>
- ⁵ A. Hussain and M. Abbas, *J. Modern Nanotechnol.*, **1**, (2021), <https://doi.org/10.53964/jmn.2021004>
- ⁶ K. Eshkobilov, S. Negmatov, S. Abed and G. Gulyamov, in *IOP Conference Series: Materials Science and Engineering*, 2021, vol. 1030, ID 012172
- ⁷ F. Hosseinali and J. A. Thomasson, *Tribol. Int.*, **127**, 433 (2018), <https://doi.org/10.1016/j.triboint.2018.06.029>
- ⁸ Y. Zhang, Y. Tian and Y. Meng, *Sci. Rep.*, **6**, 25403 (2016), <https://doi.org/10.1038/srep25403>
- ⁹ R. Chen, J. Ye and W. Zhang, *Friction*, **9**, 1050 (2021), <https://doi.org/10.1007/s40544-020-0398-8>
- ¹⁰ C. Zhang, K. D. Sinan and C. Dominique, *Carbohydr. Polym.*, **258**, 117682 (2021), <https://doi.org/10.1016/j.carbpol.2021.117682>
- ¹¹ S. A. Bochkareva, S. V. Panin, B. A. Lyukshin, P. A. Lyukshin and V. O. Aleksenko, *Phys. Mesomech.*, **23**, 147 (2020), <https://doi.org/10.1134/S102995992002006X>
- ¹² R. M. Muthoka, H. C. Kim, J. W. Kim, L. Zhai, P. S. Panicker *et al.*, *Materials*, **13**, 710 (2020), <https://doi.org/10.3390/ma13030710>.
- ¹³ J. A. Sánchez-Badillo, M. Gallo, J. G. Rutiaga-Quiñones and P. López-Albarrán, *Cellulose*, **28**, 6767 (2021), <https://doi.org/10.1007/s10570-021-03992-7>
- ¹⁴ S. Huang, X. Wu and P. Li, *Fibres Text. East. Eur.*, **29**, 32 (2021), <https://doi.org/10.5604/01.3001.0015.2719>
- ¹⁵ S. Tsuneyuki, *Acta Cryst. A, Found. Adv.*, **A49** Supplement, C5 (1993), <https://doi.org/10.1107/S0108767378099845>
- ¹⁶ I. Leven, H. Hao, S. Tan, X. Guan, K. A. Penrod *et al.*, *J. Chem. Theory Comput.*, **17**, 3237 (2021), <https://doi.org/10.1021/ACS.JCTC.1C00118>
- ¹⁷ H. H. Seung, H. Liu and A. V. Duin, *J. Am. Ceram. Soc.*, **103**, 3060 (2020), <https://doi.org/10.1111/jace.17008>
- ¹⁸ M. Wang, F. L. Duan and X. Mu, *Langmuir*, **35**, 5463 (2019), <https://doi.org/10.1021/acs.langmuir.8b04291>
- ¹⁹ Y. Dong, Q. Li, J. Wu and A. Martini, *Model. Simul. Mater. Sci. Eng.*, **19**, 065003 (2011), <https://doi.org/10.1088/0965-0393/19/6/065003>
- ²⁰ Y. Dong, *Tribol. Lett.*, **44**, 367 (2011), <https://doi.org/10.1007/s11249-011-9850-2>

- ²¹ A. C. T. van Duin, S. Dasgupta, F. Lorant and W. A. Goddard, *J. Phys. Chem. A*, **105**, 9396 (2001), <https://doi.org/10.1021/jp004368u>
- ²² K. S. Yun, H. Kwak, A. V. Vasenkov, D. Sengupta and A. V. Duin, *ACS Catal.*, **5**, 7226 (2015), <https://doi.org/10.1021/acscatal.5b01766>
- ²³ A. V. Duin, A. Alejandro, S. Shannon, Q. Zhang, X. Xu *et al.*, *ACS Catal.*, **107**, 3803 (2003), <https://doi.org/10.1021/jp0276303>
- ²⁴ X. Zhang, PhD Thesis, Northeast Forestry University, Harbin, (2013), <https://kns.cnki.net/KCMS/detail/detail.aspx?dbname=CDFD1214&filename=1013359151.nh>
- ²⁵ P. J. Flory, *Phys. Today*, **23**, 5, 71 (1978), <https://doi.org/10.1021/ma00008a013>
- ²⁶ K. Mazeau and L. Heux, *J. Phys. Chem. B*, **107**, 2394 (2008), <https://doi.org/10.1021/jp0219395>
- ²⁷ W. Chen, G. C. Lickfield and C. Yang, *Polymer*, **45**, 7357 (2004), <https://doi.org/10.1016/j.polymer.2004.08.023>
- ²⁸ H. E. Swanson, R. K. Fuyat and G. M. Ugrinic, *Phys. Today*, **7**, 22 (1954), <https://doi.org/10.1063/1.3061729>
- ²⁹ M. P. Florian, *ChemPhysChem*, **3**, 754 (2002), [https://doi.org/10.1002/1439-7641\(20020916\)3:93.O.C O;2-U](https://doi.org/10.1002/1439-7641(20020916)3:93.O.C O;2-U)
- ³⁰ Y. Zhang, W. Wang and J. Liao, *Trans. Chin. Soc. Agric. Eng.*, **33**, 45 (2017), <https://doi.org/10.11975/j.issn.1002-6819.2017.18.006>
- ³¹ T. Schneider and E. Stoll, *Phys. Rev.*, **17**, 1302 (1978), <https://doi.org/10.1103/PhysRevB.17.1302>
- ³² Y. Zhang, S. Luo and H. Zhang, *Noise Vibr. Control*, **37**, 41 (2017), <https://doi.org/10.3969/j.issn.1006-1355.2017.06.008>
- ³³ S. Plimpton, *J. Comput. Phys.*, **117**, 1 (1995), <https://doi.org/10.1006/jcph.1995.1039>
- ³⁴ A. Stukowski, *Model. Simul. Mater. Sci. Eng.*, **18**, 2154 (2010), <https://doi.org/10.1088/0965-0393/18/1/015012>